Loss of Omi mitochondrial protease activity causes the neuromuscular disorder of *mnd2* mutant mice

Julie M. Jones[1], Pinaki Datta[4], Srinivasa M. Srinivasula[4], Weizhen Ji[1], Sanjeev Gupta[4], ZhiJia Zhang[4], Erika Davies[5], György Hajnóczky[5], Thomas L. Saunders[2], Margaret L. Van Keuren[3], Teresa Fernandes-Alnemri[4], Miriam H. Meisler[1] & Emad S. Alnemri[4]

[1]Department of Human Genetics, [2]Department of Internal Medicine, Division of Molecular Medicine and Genetics, and [3]Transgenic Animal Model Core, Biomedical Research Core Facilities, University of Michigan, Ann Arbor, Michigan 48109-0618, USA
[4]Center for Apoptosis Research and the Department of Microbiology and Immunology, Kimmel Cancer Institute, and
[5]Department of Pathology and Cell Biology, Thomas Jefferson University, Philadelphia, Pennsylvania 19107, USA

The mouse mutant *mnd2* (motor neuron degeneration 2) exhibits muscle wasting, neurodegeneration, involution of the spleen and thymus, and death by 40 days of age[1,2]. Degeneration of striatal neurons, with astrogliosis and microglia activation, begins at around 3 weeks of age, and other neurons are affected at later stages[3]. Here we have identified the *mnd2* mutation as the missense mutation Ser276Cys in the protease domain of the nuclear-encoded mitochondrial serine protease Omi (also known as HtrA2 or Prss25). Protease activity of Omi is greatly reduced in tissues of *mnd2* mice but is restored in mice rescued by a bacterial artificial chromosome transgene containing the wild-type Omi gene. Deletion of the PDZ domain partially restores protease activity to the inactive recombinant Omi protein carrying the Ser276Cys mutation, suggesting that the mutation impairs substrate access or binding to the active site pocket. Loss of Omi protease activity increases the susceptibility of mitochondria to induction of the permeability transition, and increases the sensitivity of mouse embryonic fibroblasts to stress-induced cell death. The neurodegeneration and juvenile lethality in *mnd2* mice result from this defect in mitochondrial Omi protease.

mnd2 was identified in 1990 as a spontaneous, recessively inherited mutation that arose on the C57BL/6J inbred background[1]. The earliest symptoms are altered gait and cessation of normal weight gain, followed by ataxia, repetitive movements and akinesis. Striatal neurons are most susceptible, but other neurons in the central nervous system, brain stem and spinal cord, including motor neurons, are affected at later stages[1,3]. The neuronal degeneration combines features of necrosis with features of apoptosis including nuclear condensation, TdT-mediated dUTP nick end labelling (TUNEL) staining, and DNA laddering[3]. Early degeneration of mitochondria was also noted[3].

To identify the molecular basis for the *mnd2* disorder, we crossed the mutant strain C57BL/6J-*mnd2* with CAST/Ei[2]. Analysis of 1,208 F[2] mice localized the gene to a 0.9-megabase (Mb) interval of mouse chromosome 6 (Fig. 1a). The human orthologue is located in a
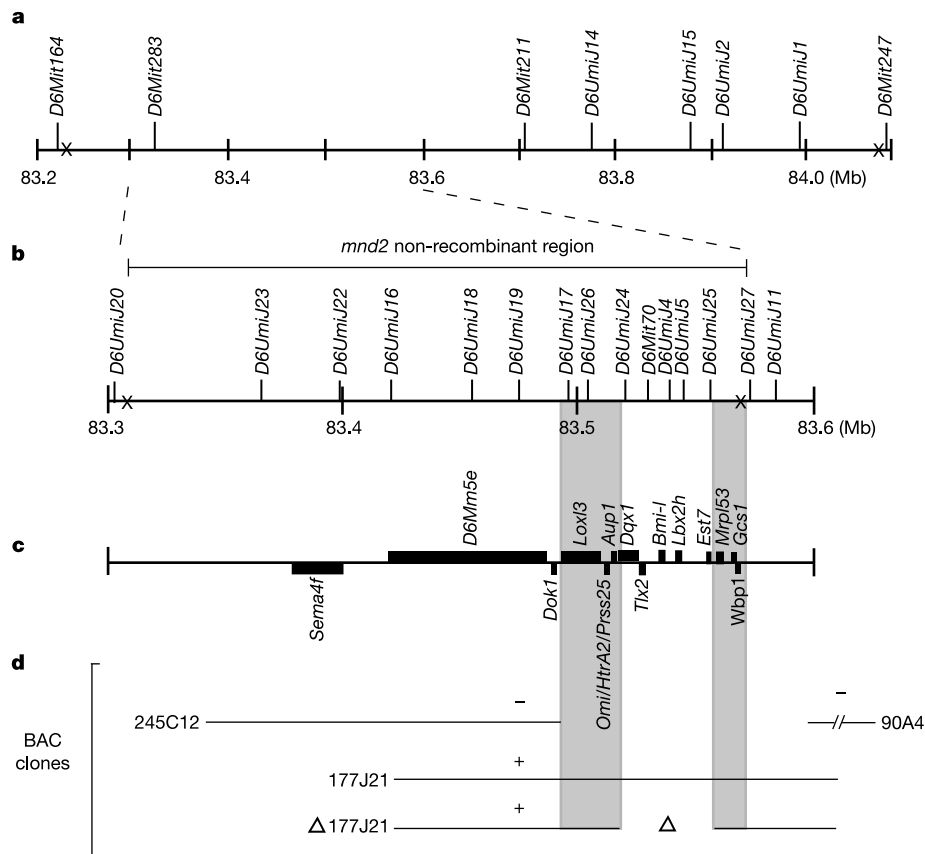

Figure 1 Genetic and physical map of the *mnd2* region. **a**, Previous non-recombinant region[2]. **b**, Reduced non-recombinant interval from the cross between C57BL/6J-*mnd2* and SJL/J mice. **c**, Gene content of the non-recombinant region. Genes above and below the horizontal line have opposite orientation on the chromosome. **d**, Overlapping BAC clones of mouse genomic DNA spanning the non-recombinant region. A plus sign indicates BACs that rescue the *mnd2* phenotype in transgenic mice; a minus sign indicates BACs that do not rescue the *mnd2* pehonotype; a triangle indicates the position of the BAC 177J21 deletion in transgenic line Tg410.

Table 1 **Transgenic rescue of *mnd2* homozygotes by expression of BAC clones**

BAC clone	Tg line	Number of rescued mice (*mnd2/mnd2*,*Tg/+*)
177J21	Tg514	21 of 21
Δ177J21	Tg410	10 of 10
90A4	Tg70	0 of 5
245C12	Tg666, 673	0 of 5

Clones are described in Fig. 1d. Each transgenic line is derived from an individual founder carrying the indicated BAC clone. Non-transgenic *mnd2/mnd2* mice are severely impaired and do not survive beyond 40 days of age. The oldest rescued mice have currently survived beyond 10 months with no phenotypic abnormalities.

gene-dense region of human chromosome 2p13 with conserved gene order and content[4]. Because of the low rate of recombination in the original cross, we initiated a second cross between strains C57BL/6J-*mnd2* and SJL/J. Recombination breakpoints in 400 F_2 mice from the second cross localized *mnd2* to an interval of 250 kilobases (kb) containing 14 genes (Fig. 1b, c).

Three BAC clones containing mouse genomic DNA spanning the non-recombinant region were tested for their ability to rescue the lethal *mnd2* phenotype (Fig. 1d). Transgenic mice carrying each BAC clone were generated by microinjection of fertilized eggs. The *mnd2* phenotype was completely corrected in transgenic line Tg514 carrying BAC clone 177J21 (Table 1). Homozygous *mnd2/mnd2*

mice carrying this transgene have normal weight gain and fertility, and do not exhibit any of the phenotypic abnormalities of the *mnd2* disorder. BAC clones 245C12 and 90A4 did not rescue *mnd2* homozygotes. In transgenic line Tg410, a deletion occurred within BAC 177J21, but the ability to rescue *mnd2* mice was retained (Table 1). The size and position of the deletion, Δ177J21, was determined by crossing the transgene onto strain SJL and testing for C57BL/6J alleles of polymorphic *D6UmiJ* markers (Fig. 1d). Combining information from the deleted BAC clone and the distal recombination breakpoint localized *mnd2* to a 40-kb region containing six candidate genes: *Loxl3*, *Omi*, *Aup1*, *Mrpl53*, *Gcs1* and *Wbp1* (Fig. 1, shaded areas).

In parallel with the mapping and rescue experiments, we compared the mutant and wild-type sequences for these six candidate genes as well as most of the other genes in the original 0.9-Mb region[4–8]. Comparison of >50 kb of gene sequences from *mnd2* and C57BL/6J identified only one difference, an A to T nucleotide substitution in exon 3 of the nuclear-encoded mitochondrial serine protease Omi (Fig. 2a). This missense mutation changes serine 276 to cysteine. Serine 276 is located in the protease domain of Omi close to serine 306, the active site serine[9], and is evolutionarily conserved in prokaryotic and eukaryotic homologues (Fig. 2b).

Omi is localized in the intermembrane space of the mitochondria[10–14] and is a member of the HtrA protease-chaperone family.
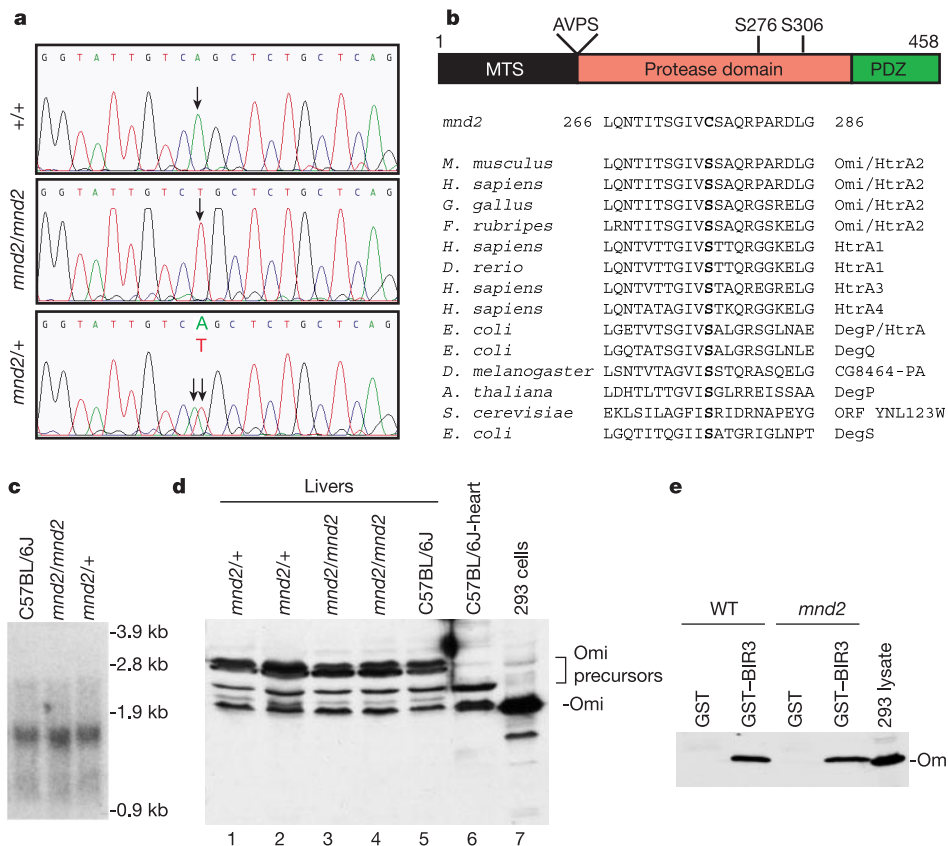

Figure 2 Ser276Cys mutation in Omi. **a**, Nucleotide sequence chromatogram from exon 3 of wild-type (top panel), *mnd2* (middle panel) and heterozygous (bottom panel) DNA. The *Prss25*[mnd2] mutation, an A to T transversion at nucleotide 826, is indicated by the arrow. **b**, Evolutionary conservation of Ser 276 in HtrA proteins. The AVPS motif at residues 134–137 binds to IAPs. Ser 276 and the active site Ser 306 in the protease domain are indicated. MTS, mitochondrial localization signal. **c**, Northern blot with 5 μg of poly(A)+ RNA was hybridized with the 0.8-kb *Eco*RI/*Not*I fragment from expressed sequence tag clone 1264040 (GenBank AA881220). **d**, Western blot of Omi protein in total liver extracts from five mice of indicated genotypes. Lanes 6 and 7 contain total extracts from wild-type mouse heart and 293T human cells, respectively. All lanes contain equal amounts of total proteins. **e**, Western blot analysis of glutathione *S*-transferase (GST)–BIR3-bound Omi proteins from wild-type and *mnd2* liver extracts. Liver extracts from wild-type (WT) or *mnd2* mice were bound to GST (GST lanes) or GST–BIR3 (GST–BIR3 lanes) fusion protein immobilized on glutathione-Sepharose beads. The beads were washed and the bound proteins were eluted with SDS sample buffer and western-blotted with anti-Omi-specific antibody. Last lane, human 293T cells.

Bacterial members are quality control proteases that are essential for surviving high temperature or oxidative stress[15,16]. Recently, Omi was shown to be released from the mitochondria with cytochrome *c* and Smac (also known as DIABLO) during apoptosis[10–14]. The released Omi can bind to inhibitors of apoptosis proteins (IAPs), inhibit their activity and directly degrade them[17,18].

The missense mutation does not alter the size or steady-state abundance of the Omi messenger RNA in *mnd2* tissues (Fig. 2c). Evaluation of the Omi protein also revealed no effect on the molecular mass or protein concentration (Fig. 2d). The precursor protein appears to be correctly processed into the mature IAP-binding form by protease cleavage of the amino terminus in mutant tissues (Fig. 2d). Binding of Omi to the Baculovirus Inhibitory Repeat 3 (BIR3) domain of X-chromosome-linked IAP (XIAP) was comparable in wild-type and mutant tissue extracts (Fig. 2e), indicating that maturation and the IAP-binding activity of Omi are not affected by the Ser276Cys substitution. To determine the effect on protease activity, Omi was immunoprecipitated from liver and assayed with ^{35}S-labelled β-casein as substrate (Fig. 3a). No β-casein cleaving activity was detectable in the immunoprecipitates from *mnd2* tissues (Fig. 3a). In livers of *mnd2/mnd2* homozygotes from lines Tg410 and Tg514, which are phenotypically rescued by BAC clones 177J21 and Δ177J21, the protease activity of Omi is restored (Fig. 3b).

The physiological concentration of Omi in highly expressing cells such as 293T cells is approximately 150 nM (Fig. 2d, lane 7; see also ref. 17). Recombinant Omi containing the Ser276Cys mutation had no detectable protease activity at concentrations of up to seven times this concentration (Fig. 3c, lane 5). A low level of residual activity was only detectable at much higher concentrations (Fig. 3c, lane 6). The mutant protein was also inactive towards the substrates XIAP and c-IAP1 (Fig. 3d).

Although the Ser276Cys mutant does not have protease activity at physiological concentrations, the results in Figs 2 and 3 indicate that it is correctly processed into the mature form. These observations suggest that processing of Omi into the mature form is probably
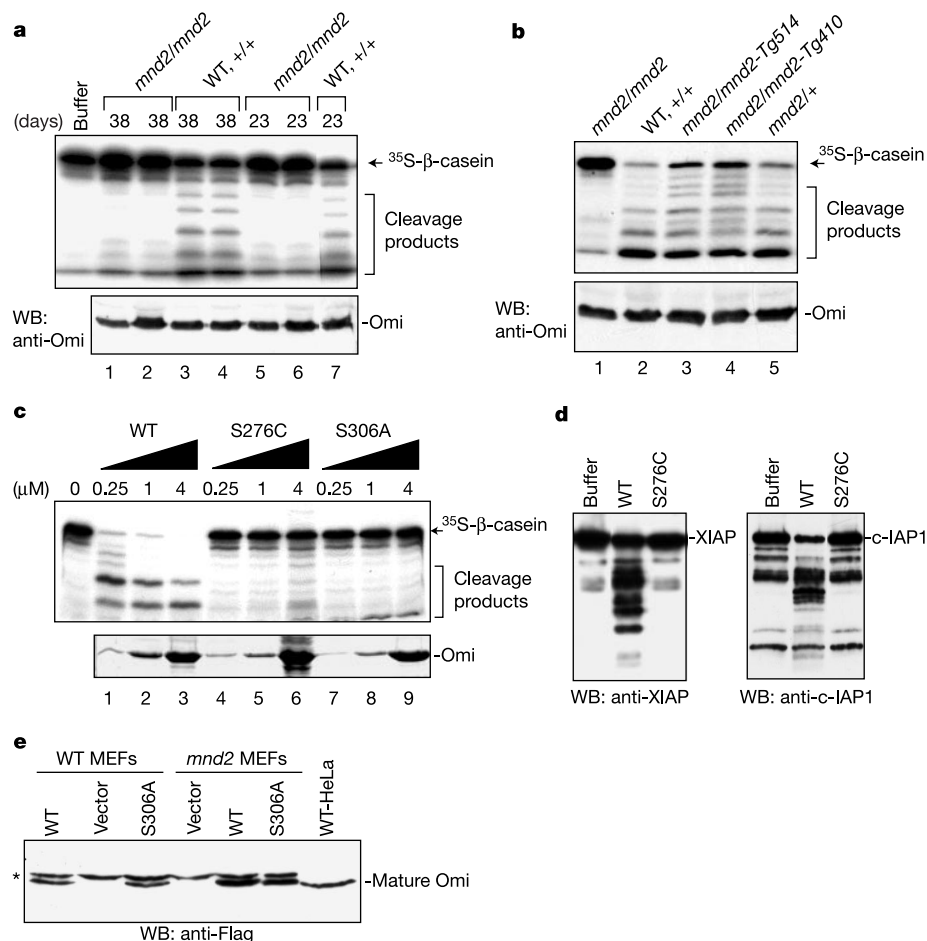

Figure 3 Effect of the Ser276Cys mutation on the protease activity of Omi. **a**, Loss of serine protease activity of Omi in *mnd2* tissues. Top panel: endogenous Omi was immunoprecipitated from liver extracts of 23- and 38-day-old mice and assayed with ^{35}S-labelled β-casein as substrate. Bottom panel: western blot of liver S100 extracts with Omi-specific polyclonal antibody demonstrating normal amounts of protein in *mnd2*. **b**, The Omi activity is restored in transgenic lines Tg514 and Tg410. **c**, Loss of activity of recombinant Omi with the Ser276Cys mutation at near physiological concentration. Top panel: ^{35}S-labelled β-casein was incubated with increasing concentrations of affinity-purified recombinant Omi. Cleavage products were analysed by SDS–PAGE and autoradiography. Bottom panel: Coomassie-stained gel of affinity-purified Omi proteins.

The active site mutant Ser306Ala lacking activity is included as control. **d**, Western blot analysis of IAP cleavage by recombinant Omi protein. Purified XIAP (left panel) or c-IAP1 (right panel) were incubated with buffer or 250 nM Omi protein. Products were separated by SDS–PAGE and immunoblotted with antibodies against XIAP or c-IAP1 as indicated. **e**, Maturation of Omi is not affected by the Ser276Cys mutation. MEFs were transfected with constructs encoding C-terminal Flag-tagged Omi precursors. At 24 h after transfection, cells were solubilized in SDS sample buffer, fractionated by SDS–PAGE, and immunoblotted with anti-Flag antibody. Last lane, lysate from HeLa cells expressing mature C-terminal Flag-tagged wild-type Omi. Asterisk, nonspecific band. The lanes labelled buffer contain substrate incubated with buffer alone.

catalysed by other mitochondrial proteases. To test this hypothesis, we overexpressed wild-type Omi and the active site mutant Ser306Ala in mouse embryonic fibroblast cells (MEFs). If Omi is involved in its own processing, then MEFs from *mnd2* mice should be less effective in processing the inactive Ser306Ala protein. No difference was observed in the extent of processing in wild-type and *mnd2* MEFs (Fig. 3e), indicating that other mitochondrial proteases are involved in maturation of Omi.

In the recently published X-ray structure of Omi, Ser 276 is located near a region critical for homotrimerization[9]. As formation of a homotrimeric complex is required for protease activity, we evaluated the effect of the mutation on trimerization. Flag- and T7-tagged Omi proteins were co-expressed in 293T cells and cell extracts were prepared. T7-tagged and endogenous Omi proteins were co-immunoprecipitated with the Flag-tagged Ser276Cys protein (Fig. 4a), indicating that the mutation does not prevent homotrimerization.

The PDZ domain in Omi restricts access of substrate to the active site pocket[9]. The location of Ser 276 in the highly flexible L3 loop, which is flanked by the PDZ domain on one side and the active site pocket on the opposite side[9,15], suggested that the Ser276Cys mutation might negatively affect the packing interactions at the interface between PDZ and protease domains, resulting in loss of access to the active site pocket. Deletion of the PDZ domain increased the activity of the wild-type protein and partially restored the protease activity of the Ser276Cys mutant (Fig. 4b). The Ser276Cys mutation may affect flexibility of the L3 loop, forcing the PDZ domain into a conformation that blocks the active site pocket of the mutant protein. Alternatively, the Ser276Cys substitution may destabilize intramolecular interactions between the PDZ and protease domains, preventing the PDZ domain from orienting the substrate into the active site pocket. Substrate binding to the

active site may also be impaired, as deletion of the PDZ domain did not fully restore protease activity.

The *mnd2* MEFs lack Omi activity (Fig. 5a). To examine the effect of loss of Omi protease activity on cell viability, *mnd2* and wild-type MEFs were treated with stress-inducing agents and subsequently stained with annexin V and propidium iodide. The proportion of stained cells was greatest in homozygous *mnd2/mnd2* MEFs (Fig. 5b), indicating increased cell death. The *mnd2* MEFs exhibited annexin V and propidium iodide staining (Fig. 5c), suggesting that both apoptosis (annexin V) and necrosis (propidium iodide) occur in these cells. This is consistent with observations of striatal neurons in *mnd2* mice, which combine aspects of apoptosis and necrosis[3]. The caspase inhibitor z-VAD-fmk did not completely inhibit death of *mnd2* MEFs (Fig. 5d), suggesting that some cell death occurs by a caspase-independent mechanism. The data indicate that loss of Omi protease activity increases sensitivity to stress-induced cell death.

Induction of the mitochondrial permeability transition can cause mitochondrial membrane permeabilization and dysfunction leading to apoptosis and necrosis[19]. To determine whether the Ser276Cys substitution in Omi affects the integrity of the mitochondrial membrane barrier, fluorimetric measurement of the mitochondrial membrane potential ($\Delta\Psi_m$) and cytosolic Ca^{2+} concentration ($[Ca^{2+}]_c$) was carried out in permeabilized MEFs after calcium pulsing. In surviving cells, Ca^{2+} is taken up by mitochondria during $[Ca^{2+}]_c$ spiking and is used to stimulate mitochondrial ATP production. However, in cells exposed to certain pro-apoptotic agents, propagation of $[Ca^{2+}]_c$ signals to the mitochondria triggers activation of the permeability transition pore (PTP) and mitochondrial membrane permeabilization, leading to execution of apoptosis[20]. In wild-type MEFs, added Ca^{2+} caused only a small and transient depolarization and was effectively removed from cytosol by the mitochondria (Fig. 6, black traces and bars). In contrast, in *mnd2* MEFs, Ca^{2+} pulsing induced relatively large and prolonged mitochondrial depolarization and a progressive rise in $[Ca^{2+}]_c$ (Fig. 6, grey traces and bars). These results suggest that *mnd2* mutant cells are more vulnerable to Ca^{2+}-induced permeability transition and mitochondrial membrane permeabilization. The Ser276Cys substitution in Omi thus seems to promote activation of the PTP by Ca^{2+}. As stress-inducing agents may also target the PTP through elevation in Ca^{2+} concentration or free radical formation, sensitization of the PTP in *mnd2* mutant cells provides a potential mechanism to explain the increased sensitivity of *mnd2* MEFs to stress-induced cell death, as well as the degeneration of striatal neurons in *mnd2* mice. Supporting this mechanism, recent studies have shown that striatal mitochondria are more vulnerable to calcium-induced permeability transition than cortical mitochondria[19]. Therefore, mitochondrial dysfunction is probably responsible for the selective death of striatal neurons in *mnd2* mice.

We have demonstrated that the Ser276Cys missense mutation in Omi is responsible for neurodegeneration in *mnd2* mutant mice. Omi is a serine protease normally present in the intermembrane space of mitochondria[10–14]. *In vitro* studies with cancer cell lines have shown that release of Omi from the mitochondria into the cytosol causes inhibition and degradation of IAPs and apoptosis[17,18]. However, there are no loss-of-function models that support a role for Omi in apoptosis *in vivo*. On the contrary, the data presented here demonstrate that loss of the protease activity of Omi increases sensitivity to stress-induced cell death and is probably responsible for the massive loss of striatal neurons in *mnd2* mutant mice[3]. The data can be explained if Omi has two distinct functions: (1) under normal physiological conditions it is required within mitochondria for maintenance of mitochondrial homeostasis, and (2) under apoptotic conditions it is released from mitochondria and has an apoptotic role that is shared by other released proteins such as cytochrome *c* (ref. 21) and apoptosis-inducing factor (AIF)[22,23]. We
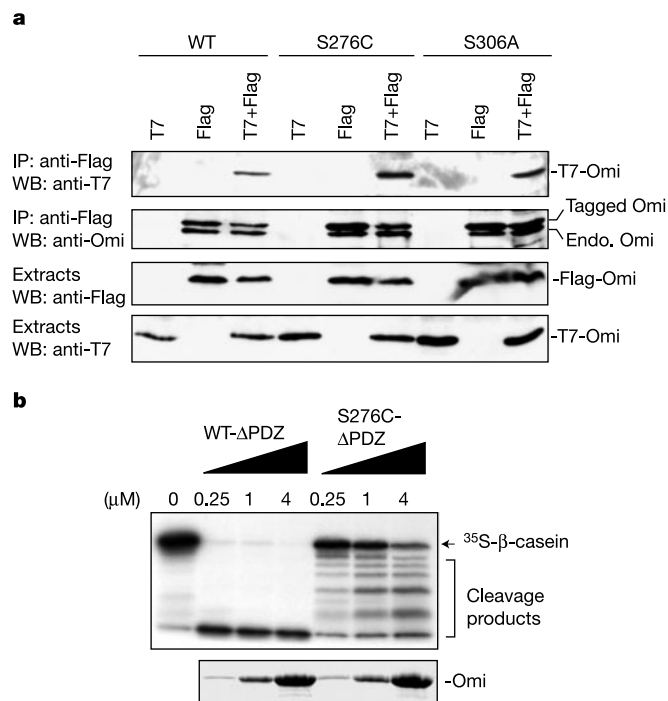
Figure 4 Structural determinants of Omi activity. **a**, The Ser276Cys mutation does not affect homotrimerization. (For assay conditions, see Methods section.) **b**, Deletion of the PDZ domain partially restores the protease activity of the Ser276Cys Omi mutant. The activity of the PDZ-deleted Omi proteins was determined as in Fig. 3c. Wild-type PDZ-deleted protein catalysed the complete digestion of substrate.

propose that the Ser276Cys mutation compromises the mitochondrial function, leading to mitochondrial membrane permeabilization and cytoplasmic release of mutant Omi along with other active inducers of cell death.

The structural similarity between Omi and bacterial HtrA proteins[15,16,24] suggests that Omi may be a sensor of unfolding stresses in the mitochondria. Thus, loss of Omi protease activity in the *mnd2* mice could lead to accumulation of misfolded and damaged proteins in the mitochondria, increased susceptibility to induction of the permeability transition and mitochondrial dysfunction. Progressive mitochondrial dysfunction can lead to irreversible loss of neuronal cells, and this is thought to be an important pathogenic mechanism in many neurodegenerative disorders. Mitochondrial disintegration is an early component of neuronal degeneration in the striatum of *mnd2* mice[3]. The dying striatal neurons exhibit features of apoptosis such as condensation of nuclear DNA, nuclear shrinkage, TUNEL staining and DNA laddering[3]. Some cells also exhibit features of necrosis[3]. This neuronal degradation was not prevented by overexpression of Bcl2 (ref. 3). The loss of protein quality control in the mitochondria can account for both types of cell death in *mnd2* mice. Induction of mitochondrial permeability

transition due to accumulation of misfolded proteins might lead to release of the mitochondrial apoptotic proteins that activate the caspase-dependent and -independent cell death cascades. At the same time, the loss of mitochondrial respiratory competence, and reduced intracellular ATP levels, might result in rupture of the plasma membrane and necrotic cell death[25].

AIF is a nuclear-encoded mitochondrial protein that is localized in the intermembrane space and is involved in apoptosis[26]. In the mouse mutant harlequin (*Hq*), AIF expression is reduced to 20% of normal, resulting in oxidative stress and degeneration of cerebellar neurons[23]. The mechanism of cell death in this mutant is loss of the hydrogen peroxide scavenger function of AIF. BAD is another protein involved in apoptosis, which has recently been shown to reside in a mitochondrial complex that integrates glycolysis and apoptosis[27]. Similar to Omi, these proteins combine an essential mitochondrial function with a role in inducing apoptosis. The human neurodegenerative disease hereditary spastic paraplegia (SPG7) is also caused by inactivation of a mitochondrial protease called paraplegin[28]. The yeast homologues of paraplegin, known as AAA proteases, are quality control protease-chaperons anchored to the inner mitochondrial membrane[29]. In both SPG7 and *mnd2* the
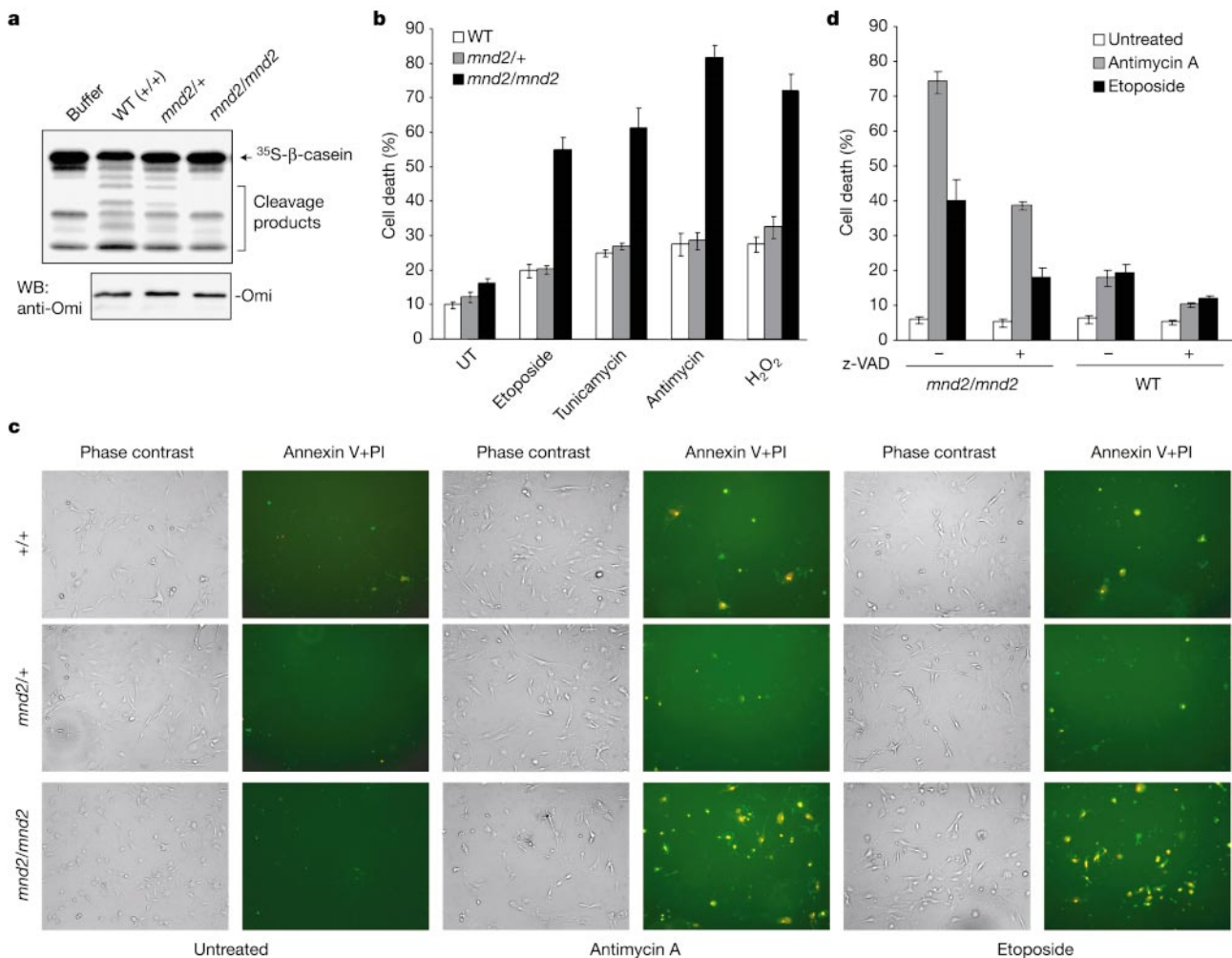

Figure 5 Sensitivity of *mnd2* MEFs to stress-induced cell death. **a**, The top panel shows protease activity of Omi in cultured MEFs. Activity was determined as in Fig. 3a. The bottom panel shows western blot of MEF extracts with Omi-specific antibody. **b**, MEFs were treated with stress-inducing agents and then stained with annexin V and propidium iodide. The percentage of cell death was determined as described in Methods. UT, untreated. **c**, Representative fields of control (untreated) MEFs and treated MEFs stained with annexin V (green fluorescence) and propidium iodide (PI, orange fluorescence). Cells were visualized by fluorescence microscopy (× 10). **d**, z-VAD-fmk partially inhibits stress-induced cell death of *mnd2* MEFs. MEFs were treated with antimycin A or etoposide in the presence (+) or absence (−) of the pan-caspase inhibitor z-VAD-fmk.
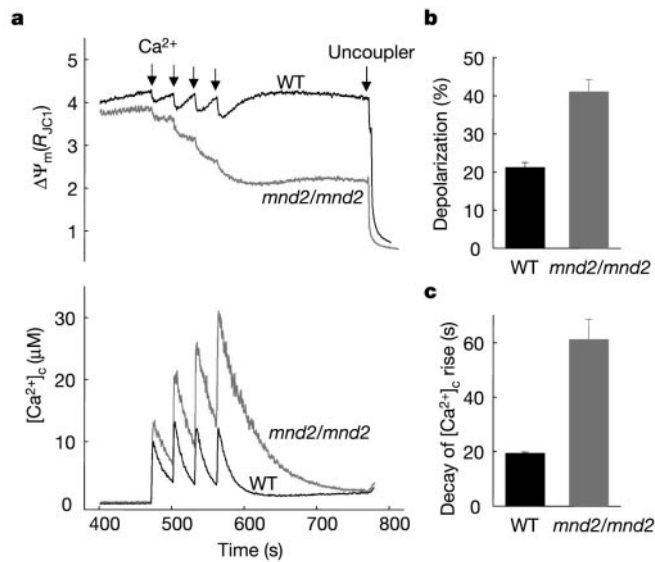
Figure 6 Ca^{2+} pulsing-induced mitochondrial membrane permeabilization in *mnd2* MEFs. **a**, $\Delta\Psi_m$ (top) and $[Ca^{2+}]_c$ (bottom) recordings from *mnd2/mnd2* (grey) and wild-type (black) MEFs. Additions: Ca^{2+}, 30 μM $CaCl_2$ at each arrow; uncoupler, 1 μM FCCP. Data are representative of 5–6 different measurements. **b**, Quantification of mitochondrial depolarization in response to Ca^{2+} pulsing. To quantify Ca^{2+}-induced depolarization, the Ca^{2+}-induced decrease in the JC1 fluorescence ratio R_{JC1} was normalized to the uncoupler-induced decrease in R_{JC1} in both *mnd2/mnd2* and wild-type MEFs. **c**, Determination of mitochondrial Ca^{2+} uptake. To evaluate mitochondrial Ca^{2+} uptake, the duration at half maximum of the $[Ca^{2+}]_c$ transient evoked by the fourth Ca^{2+} pulse was calculated. Data from separate experiments are shown as mean ± s.e.m.

cause of mitochondrial dysfunction and neurodegeneration may include defective protein quality control, in the mitochondrial matrix or intermembrane space, respectively. It remains to be seen whether spontaneous mutations in Omi are responsible for neuro-degeneration disorders in humans.

Note added in proof: The human *OMI* gene is located near the Parkinson's disease susceptibility locus *PARK3* on chromosome 2p13.1. No coding or splice site mutations of human OMI were detected in two families with Parkinson's disease mapped to the *PARK3* locus (J.M.J., S.M.S., T.F.-A., M.H.M. and E.S.A., unpublished observations). □

Methods

Animals
The *mnd2* mutation arose on strain C57BL/6J in 1990 at the University of Michigan. C57BL/6J-*mnd2*/+ males were mated with SJL/J females. The F_1 offspring were test-crossed with C57BL/6J-*mnd2*/+ mice. Confirmed heterozygotes were intercrossed to generate F_2 mice. C57BL/6J and SJL/J mice were obtained from the Jackson Laboratory.

BAC transgenic mice
BAC clones RP23-177J21 and RP23-90A4 were obtained from BAC/PAC resources (Oakland Children's Hospital); clone 245C12 has been described previously[2]. DNA from BAC clones was purified with Nucleobond columns (BD Biosciences-ClonTech) (http://www.med.umich.edu/tamc/BACnucleo.html). Female F_2 heterozygotes from the SJL cross were superovulated and mated with F_1 heterozygous males to generate fertilized eggs for microinjection. Transgenic founders were identified by polymerase chain reaction (PCR) amplification of tail DNA using BAC-specific primers flanking each vector-insert junction. The integrity of the BAC transgenes 177J21 and 90A4 were analysed by crossing onto a homozygous SJL/J background and detection of C57BL/6J alleles of the appropriate *D6UmiJ* markers (Fig. 1a, b). The integrity of BAC 245C12 was evaluated by detection of alleles from strain 129/Sv on a C57BL/6J background.

Markers and genotyping
Nineteen new genetic markers, *D6UmiJ1* to *D6UmiJ27*, with different alleles in C57BL/6J and SJL/J were generated using primers flanking microsatellite sequences in the C57BL/6J genome. Primer sequences and allele sizes are available from the Mouse Genome Database (www.informatics.jax.org). The Ser276Cys mutant allele of Omi, designated *Prss25*[*mnd2*], is

detected by amplification of a 500-base pair (bp) fragment containing exon 3 from genomic DNA using the primers mnd2F (5′-CACACTGAGGGATTCAAACCAAGGT-3′) and mnd2R (5′-GACCGAGGACATAAACAGGGTGTA-3′). Digestion with *Alu*I produces a 244-bp product from the mutant allele in place of wild-type fragments of 171 bp and 73 bp. PCR of genomic DNA was carried out using the primers described in the text, in a volume of 25 μl containing × 1 Taq DNA polymerase buffer (Promega), 2.5 mM $MgCl_2$, 0.2 mM dNTPs, 0.5 μM primers and 1 U Taq DNA polymerase in storage buffer B (Promega). Incubation at 94 °C for 2 min was followed by 34 cycles of 94 °C for 45 s, 60 °C for 45 s, and 72 °C for 45 s, followed by 72 °C for 10 min. PCR products were separated on 2% agarose gels and stained with ethidium bromide.

DNA sequence
The DNA sequences of BAC clones RP23-177J21 and b245C12 are described in GenBank under accession numbers AC104324 and AC003061, respectively. Exons of positional candidate genes were amplified from wild-type and *mnd2/mnd2* samples by PCR or PCR with reverse transcription (RT) and sequenced by the University of Michigan DNA Sequencing Core.

Complementary DNA cloning and recombinant protein expression
The wild-type full-length mouse Omi cDNA clone (GenBank AF175324) was obtained from A. Zervos. Constructs encoding wild-type and mutant full-length and mature Omi proteins were generated by PCR and overlapping PCR, using modified complementary PCR adaptor-primers. Carboxy-terminal Flag, T7 or (His)6 tagging was carried out by cloning the PCR-generated cDNAs in-frame into Flag-C-pcDNA3, T7-C-pcDNA3 or pET-21 expression vectors respectively. The human β-casein cDNA was isolated from human placenta by RT–PCR and cloned into pcDNA3 to generate the pcDNA-β-casein plasmid. All expression constructs were sequenced by the Kimmel Cancer Institute DNA sequencing core. Mature mouse Omi was overexpressed in *Escherichia coli* strain BL21(DE3) as a C-terminally (His)6-tagged protein using a pET-21 vector. ^{35}S-labelled β-casein protein was prepared by *in vitro* translation in the presence of ^{35}S-methionine using the TNT rabbit reticulocyte lysate kit from Promega. XIAP and c-IAP1 were expressed in bacteria as described[10,17].

GST–BIR3 pull-down assay
This assay was performed essentially as described[10].

Protease assay
The protease activity of recombinant wild-type and mutant Omi was assayed with the substrates ^{35}S-labelled β-casein, c-IAP1 or XIAP as described previously[17]. Different amounts of bacterially expressed (His)6-tagged Omi was purified on Talon affinity resins and then incubated with ^{35}S-labelled β-casein or IAPs in an assay buffer containing 25 mM Tris, pH 7.6, 100 mM NaCl, 250 mM imidazole and 1 mM dithiothreitol for 1 h at 37 °C in a total 50-μl reaction. Cleavage products were analysed by SDS–polyacrylamide gel electrophoresis (PAGE) and visualized by autoradiography or western blotting.

Endogenous Omi proteins were isolated by immunoprecipitation before protease assay. Frozen livers from *mnd2* and control mice were homogenized in a buffer containing 50 mM Tris, pH 7.6, 150 mM NaCl, 0.1% NP-40 and protease inhibitors, and centrifuged at 20,000*g*. The supernatants were further centrifuged at 100,000*g* and the resulting S100 extracts were incubated with an Omi-specific polyclonal antibody[17] for 1 h. After incubation, the Omi–antibody complexes were bound to protein G Sepharose and washed several times. The protein G Sepharose-bound complexes were incubated with ^{35}S-labelled β-casein in an assay buffer (25 mM HEPES, pH 7.6, 10 mM KCl, 1.5 mM $MgCl_2$, 1 mM EDTA, 1 mM EGTA) for 1 h at 37 °C in a total 50 μl reaction. Cleavage products were analysed by SDS–PAGE and visualized by autoradiography. Omi activity in MEFs was assayed by the same method.

Trimerization assay
293T cells were co-transfected with constructs encoding C-terminal Flag-tagged and T7-tagged Omi variants (wild type, S276C, S306A) using the Lipofectamine method. At 36 h after transfection, cells were lysed and the cellular lysates were immunoprecipitated with a Flag-specific antibody. The immunoprecipitates were analysed by western blotting with a T7-specific or Omi-specific antibodies.

Cell death assay
MEFs were grown in DMEM supplemented with 10% FBS and penicillin/streptomycin. MEFs were seeded in 12-well plates at a density of 5×10^4 cells per well and treated with antimycin A (100 μg ml^{-1} for 12 h), hydrogen peroxide (3 μM for 5 h), etoposide (100 μg ml^{-1} for 12 h), or tunicamycin (2.5 μg ml^{-1} for 12 h) in the presence or absence of z-VAD-fmk (50 μM). Cells were stained with annexin V and propidium iodide (CLONTECH Laboratories) as per the manufacturer's recommendations and counted. Normal and dead cells (annexin V and/or propidium iodide positive) were counted using fluorescence microscopy. The percentage of dead cells in each experiment was expressed as the mean percentage of dead cells as a fraction of the total number of cells counted. Data represent mean values from three experiments.

$\Delta\Psi_m$ and $[Ca^{2+}]_c$ assay
Measurement of $\Delta\Psi_m$ and $[Ca^{2+}]_c$ in permeabilized MEFs was carried out as described previously[20]. Equal aliquots of cells (2.4 mg protein) were resuspended and permeabilized with 40 μg ml^{-1} digitonin in 1.5 ml of an intracellular medium composed of 120 mM KCl, 10 mM NaCl, 1 mM KH_2PO_4, 20 mM HEPES/Tris, pH 7.2 supplemented with 1 μg ml^{-1} of each of the following: antipain, leupeptin, pepstatin. Measurements were carried out in

the presence of 2 mM MgATP, 5 mM phosphocreatine, 5 U ml^{-1} creatine kinase and 2 mM succinate.

To carry out simultaneous measurements of $[Ca^{2+}]_c$ and $\Delta\Psi_m$, the permeabilized cells were supplemented with 0.5 µM fura2FF/FA and 800 nM JC1. Fluorescence was monitored in a multi-wavelength-excitation dual wavelength-emission fluorimeter (DeltaRAM, PTI) using 340- and 380-nm excitation and 535-nm emission for fura2FF whereas 490-nm excitation/535-nm emission and 570-nm excitation/595-nm emission were used for JC1. $\Delta\Psi_m$ is shown as the ratio of the fluorescence of J-aggregate (excitation 570 nm/emission 595 nm) and monomer (excitation 490 nm/emission 535 nm) forms of JC1. Calibration of fura2FF signal was carried out by adding $CaCl_2$ (2.5 mM) and subsequently EGTA/Tris (10 mM) at pH 8.5. Experiments were carried out at 35 °C and with simultaneous stirring.

1. Jones, J. M. et al. mnd2: a new mouse model of inherited motor neuron disease. Genomics 16, 669–677 (1993).
2. Weber, J. S. et al. High-resolution genetic, physical, and transcript map of the mnd2 region of mouse chromosome 6. Genomics 54, 107–115 (1998).
3. Rathke-Hartlieb, S. et al. Progressive loss of striatal neurons causes motor dysfunction in MND2 mutant mice and is not prevented by Bcl-2. Exp. Neurol. 175, 87–97 (2002).
4. Jang, W. et al. Comparative sequence of human and mouse BAC clones from the mnd2 region of chromosome 2p13. Genome Res. 9, 53–61 (1999).
5. Jang, W., Weber, J. S., Bashir, R., Bushby, K. & Meisler, M. H. Aup1, a novel gene on mouse chromosome 6 and human chromosome 2p13. Genomics 36, 366–368 (1996).
6. Jang, W., Weber, J. S., Harkins, E. B. & Meisler, M. H. Localization of the rhotekin gene RTKN on the physical maps of mouse chromosome 6 and human chromosome 2p13 and exclusion as a candidate for mnd2 and LGMD2B. Genomics 40, 506–507 (1997).
7. Jang, W., Weber, J. S., Tokito, M. K., Holzbaur, E. L. & Meisler, M. H. Mouse p150Glued (dynactin 1) cDNA sequence and evaluation as a candidate for the neuromuscular disease mutation mnd2. Biochem. Biophys. Res. Commun. 231, 344–347 (1997).
8. Ji, W. et al. DQX1, an RNA-dependent ATPase homolog with a novel DEAQ box: expression pattern and genomic sequence comparison of the human and mouse genes. Mamm. Genome 12, 456–461 (2001).
9. Li, W. et al. Structural insights into the pro-apoptotic function of mitochondrial serine protease HtrA2/Omi. Nature Struct. Biol. 9, 436–441 (2002).
10. Hegde, R. et al. Identification of Omi/HtrA2 as a mitochondrial apoptotic serine protease that disrupts inhibitor of apoptosis protein-caspase interaction. J. Biol. Chem. 277, 432–438 (2002).
11. Suzuki, Y. et al. A serine protease, HtrA2, is released from the mitochondria and interacts with XIAP, inducing cell death. Mol. Cell 8, 613–621 (2001).
12. Verhagen, A. M. et al. HtrA2 promotes cell death through its serine protease activity and its ability to antagonize inhibitor of apoptosis proteins. J. Biol. Chem. 277, 445–454 (2002).
13. Martins, L. M. et al. The serine protease Omi/HtrA2 regulates apoptosis by binding XIAP through a reaper-like motif. J. Biol. Chem. 277, 439–444 (2002).
14. van Loo, G. et al. The serine protease Omi/HtrA2 is released from mitochondria during apoptosis. Omi interacts with caspase-inhibitor XIAP and induces enhanced caspase activity. Cell Death Differ. 9, 20–26 (2002).
15. Clausen, T., Southan, C. & Ehrmann, M. The HtrA family of proteases: implications for protein composition and cell fate. Mol. Cell 10, 443–455 (2002).
16. Maurizi, M. R. Love it or cleave it: tough choices in protein quality control. Nature Struct. Biol. 9, 410–412 (2002).
17. Srinivasula, S. M. et al. Inhibitor of apoptosis proteins are substrates for the mitochondrial serine protease Omi/HtrA2. J. Biol. Chem. 278, 31469–31472 (2003).
18. Yang, Q. H., Church-Hajduk, R., Ren, J., Newton, M. L. & Du, C. Omi/HtrA2 catalytic cleavage of inhibitor of apoptosis (IAP) irreversibly inactivates IAPs and facilitates caspase activity in apoptosis. Genes Dev. 17, 1487–1496 (2003).
19. Brustovetsky, N. et al. Increased susceptibility of striatal mitochondria to calcium-induced permeability transition. J. Neurosci. 23, 4858–4867 (2003).
20. Szalai, G., Krishnamurthy, R. & Hajnoczky, G. Apoptosis driven by IP(3)-linked mitochondrial calcium signals. EMBO J. 18, 6349–6361 (1999).
21. Reed, J. C. Cytochrome c: can't live with it—can't live without it. Cell 91, 559–562 (1997).
22. Joza, N. et al. Essential role of the mitochondrial apoptosis-inducing factor in programmed cell death. Nature 410, 549–554 (2001).
23. Klein, J. A. et al. The harlequin mouse mutation downregulates apoptosis-inducing factor. Nature 419, 367–374 (2002).
24. Walsh, N. P., Alba, B. M., Bose, B., Gross, C. A. & Sauer, R. T. OMP peptide signals initiate the envelope-stress response by activating DegS protease via relief of inhibition mediated by its PDZ domain. Cell 113, 61–71 (2003).
25. Leist, M., Single, B., Castoldi, A. F., Kuhnle, S. & Nicotera, P. Intracellular adenosine triphosphate (ATP) concentration: a switch in the decision between apoptosis and necrosis. J. Exp. Med. 185, 1481–1486 (1997).
26. Susin, S. A. et al. Molecular characterization of mitochondrial apoptosis-inducing factor. Nature 397, 441–444 (1999).
27. Danial, N. N. et al. BAD and glucokinase reside in a mitochondrial complex that integrates glycolysis and apoptosis. Nature 424, 952–956 (2003).
28. Casari, G. et al. Spastic paraplegia and OXPHOS impairment caused by mutations in paraplegin, a nuclear-encoded mitochondrial metalloprotease. Cell 93, 973–983 (1998).
29. Van Dyck, L. & Langer, T. ATP-dependent proteases controlling mitochondrial function in the yeast Saccharomyces cerevisiae. Cell. Mol. Life Sci. 56, 825–842 (1999).

....

Functional cloning of TUG as a regulator of GLUT4 glucose transporter trafficking

Jonathan S. Bogan[1,2,3]*, Natalie Hendon[1,2], Adrienne E. McKee[1]*, Tsu-Shuen Tsao[1] & Harvey F. Lodish[1,4]

[1]Whitehead Institute for Biomedical Research, Cambridge, Massachusetts 02142, USA
[2]Diabetes Unit, Department of Medicine, Massachusetts General Hospital, Boston, Massachusetts 02129, USA
[3]Department of Medicine, Harvard Medical School, Boston, Massachusetts 02114, USA
[4]Department of Biology, Massachusetts Institute of Technology, Cambridge, Massachusetts 02142, USA

* Present addresses: Section of Endocrinology and Metabolism, Department of Internal Medicine, Yale University School of Medicine, 333 Cedar Street, Box 208020, New Haven, Connecticut 06520-8020, USA (J.S.B.); Program in Biological and Biomedical Sciences, Harvard Medical School, 220 Longwood Ave, Boston, Massachusetts 02115, USA (A.E.M.)

Insulin stimulates glucose uptake in fat and muscle by mobilizing the GLUT4 glucose transporter. GLUT4 is sequestered intracellularly in the absence of insulin, and is redistributed to the plasma membrane within minutes of insulin stimulation[1,2]. But the trafficking mechanisms that control GLUT4 sequestration have remained elusive. Here we describe a functional screen to identify proteins that modulate GLUT4 distribution, and identify TUG as a putative tether, containing a UBX domain, for GLUT4. In truncated form, TUG acts in a dominant-negative manner to inhibit insulin-stimulated GLUT4 redistribution in Chinese hamster ovary cells and 3T3-L1 adipocytes. Full-length TUG forms a complex specifically with GLUT4; in 3T3-L1 adipocytes, this complex is present in unstimulated cells and is largely disassembled by insulin. Endogenous TUG is localized with the insulin-mobilizable pool of GLUT4 in unstimulated 3T3-L1 adipocytes, and is not mobilized to the plasma membrane by insulin. Distinct regions of TUG are required to bind GLUT4 and to retain GLUT4 intracellularly in transfected, non-adipose cells. Our data suggest that TUG traps endocytosed GLUT4 and tethers it intracellularly, and that insulin mobilizes this pool of retained GLUT4 by releasing this tether.

The proportion of GLUT4 at the surface of individual living cells was assayed by using flow cytometry to measure fluorescence intensities corresponding to cell surface and total GLUT4. For this, we used a previously described GLUT4 reporter protein containing epitope tags in its first extracellular domain and green fluorescent protein (GFP) at the carboxy terminus[3]. To identify proteins that alter GLUT4 distribution, we constructed a 3T3-L1 adipocyte complementary DNA library in a retroviral vector. We used the pMX-IRES-CD2 vector because it produces a bicistronic